Biochemical and Biophysical Research Communications 422 (2012) 305–310

Contents lists available at SciVerse ScienceDirect

Biochemical and Biophysical Research Communications

journal homepage: www.elsevier.com/locate/ybbrc

A422T mutation in HERG potassium channel retained in ER is rescurable by pharmacologic or molecular chaperones

Jia Guo [a,c], XiangMei Zhang [a], ZhenSheng Hu [a], Zhong Zhuang [a], ZhongHua Zhu [a], Zhong Chen [a], Wen Chen [a], ZhongZhong Zhao [a], ChaoYing Zhang [a], Zhao Zhang [a,b,*]

[a] Jiangsu Key Laboratory for Molecular and Medical Biotechnology, College of Life Science, Nanjing Normal University, Nanjing 210046, China
[b] Jiangsu Key Laboratory for Supermolecular Medicinal Materials & Applications, College of Life Science, Nanjing Normal University, Nanjing 210046, China
[c] Department of Nephrology, the First Affiliated Hospital, Zhengzhou University, Zhengzhou 450052, China

ARTICLE INFO

Article history:
Received 24 April 2012
Available online 3 May 2012

Keywords:
Potassium channel
HERG
Long QT syndrome
Patch clamp
Protein trafficking

ABSTRACT

In the present study, we characterized biologic and electrophysiologic consequences of A422T mutation in HERG K^+ channel and the role of pharmacologic or molecular chaperons by employing a heterogeneous expression system in HEK 293 cells. It was found that A422T mutation led to a marked decrease in whole-cell recording currents, and that a complexly glycosylated form protein band at 155 kDa was missing by Western blotting analysis compared to wild type (WT). And the mutant protein was mainly located in the cytoplasm as illustrated in immunocytochemical assay, indicating that the mutation underwent a trafficking defect. In addition, A422T mutation exerted remarkable dominant-negative suppression on WT, resulting in the alteration in the kinetic processes. Strikingly, trafficking-deficient A422T mutation was partially rescued by incubating the cells at a lower temperature, administration of pharmacologic chaperon, E4031 or overexpression of a chaperon molecule, Hsp90, but not Hsp70. In conclusion, missense A422T mutation in HERG K^+ channel results in its trafficking defect, which is rescurable by pharmacologic or molecular chaperones.

1. Background

The human-ether-a-go-go-related gene (HERG) encodes the pore-forming α subunit of K^+ channel that resembles the rapid component of delayed rectifier current I_{Kr} in cardiac myocytes and non-cardiac cells [1]. Mutations in HERG cause chromosome 7-linked long QT syndrome type 2 (LQT2) [2], which is characterized by a prolonged QT interval on electrocardiogram (ECG) and predisposition to life-threatening ventricular tachyarrhythmia (i.e. torsades de pointes) that may lead to syncope and sudden death. The studies have identified 300 different mutations in HERG from LQT2 patients hitherto [3], resulting in dysfunction of HERG channels. But mutations located in different regions exhibit disparate effects on the biologic characteristics of HERG channels [4]. Thus, each mutation needs to be studied individually to further clarify the mechanisms of HERG channel dysfunction.

In the previous study [5], A422T, a missense mutation (substitution of alanine to threonine at position 422) in the S1 segment of HERG protein has been identified in a Chinese LQT2 patient. Cells co-expressed A422T and hMiRP1 (human Mink related peptide 1), which was considered to reconstitute native I_{Kr} upon coexpression with HERG [6] produced nonfunctional channels accompanied with dominant negative effects on WT channels as revealed by an electrophysiologic study. In the present study, we further characterized the biologic and electrophysiologic consequences of A422T mutation and the role of pharmacologic or molecular chaperons by employing a heterogeneous expression system in HEK 293 cells.

2. Methods

2.1. Cell culture

HEK 293 cells were cultured as previous described [7]. HEK 293 cells were transiently transfected with HERG cDNA (pCMV-GFP-HERG, kindly presented by Dr. Nipavan Chiamvimonvat, University of California, Davis, USA), or co-transfected with HERG cDNA and Hsp70 or Hsp90 cDNA (pCDNA3-Hsp70 or pCDNA3-Hsp90, kindly provided by Dr. Zhimin Yin, Nanjing Normal University, Nanjing, China). The transfection was performed by Lipofectamine™ 2000 according to the manufacturer's instruction (Invitrogen, Carlsbad, CA, USA). 36–48 h after transfection, cells were used for current recording, western blot analysis or co-immunoprecipitation assays.

* Corresponding author at: 1# Wenyuan Road, Nanjing 210046, China. Fax: +86 25 85891353.
E-mail address: zhangzhaolab@163.com (Z. Zhang).

0006-291X/$ - see front matter © 2012 Elsevier Inc. All rights reserved.
http://dx.doi.org/10.1016/j.bbrc.2012.04.153

2.2. Electropysiological recordings and data analysis

GFP-positive cells were visually selected with an epifluorescence system. The cells were superfused with bath solution containing 140 mM NaCl, 5.4 mM KCl, 1 mM $MgCl_2$, 10 mM HEPES, 10 mM glucose, 2 mM $CaCl_2$ (pH of 7.4). The internal dialysis solution contained 140 mM KCl, 1 mM $MgCl_2$, 10 mM HEPES, 4 mM K-ATP, 5 mM EGTA (pH of 7.2). The 'pipette-to-bath' liquid junction potential was measured for this filling solution to be 2.7 mV. As this value was small, no correction of membrane potential was made. HERG K^+ currents were recorded using the whole-cell configuration of patch-clamp technique at room temperature (22 ± 1 °C) as previously described [8]. Voltage commands and data acquisition were controlled by pClamp (v10.0) software, which controlled Axon 200B patch-clamp amplifier through a digitizer (DigiData 1440A, Molecular Devices, Sunnyvale, CA, USA).

2.3. Western Blot analysis

Western blot analysis of HERG protein was performed as Liu et al. described [9]. Briefly, 48 h after transfection, HERG-expressed HEK 293 cells were solubilized in ice-cold NP-40 buffer (20 mM Tris–HCl at pH 8.0, 137 mM NaCl, 10% glycerol, 1% NP-40, and 2 mM EDTA) with addition of a protease inhibitor cocktail (Roche, IN, USA). Proteins were separated on 8% SDS polyacrylamide gel, and transferred to polyvinylidene difluoride (PVDF) membranes. The primary or secondary antibodies was polyclonal rabbit anti-HERG antibodies (1:300 dilutions, Alomone, Israel) or horseradish alkaline phosphatase-conjugated secondary antibody. Then, the protein bands were visualized with BCIP-NBT Alkaline Phosphatase Color Development Kit (BOSTER, China) according to manufacturer's instruction. Blots were analyzed by desitometry using Image J software (National Institutes of Health, USA).

2.4. Confocal microscopy examination

HEK 293 cells were transfected with different HERG plasmids (pCDNA3-WT-HERG and pCDNA3-A422T-HERG, kindly gifted by Dr. Gail A. Robertson, University of Wisconsin, Madison, WI, USA). 48 h later, HEK 293 cells were fixed in 4% paraformaldehyde, treated with 0.1% Triton X-100, and blocked with 3% bovine serum albumin (BSA) at room temperature. These cells were then stained with rabbit polyclonal anti-HERG (1:50 dilution, Alomone, Israel) and mouse monoclonal anti-calnexin (1:100 dilution, Abcam, MA, USA) at 4 °C for overnight, followed by incubation with Alexa Flour 488 goat anti-rabbit IgG (H + L) and Alexa Flour 555 goat anti-mouse IgG (H + L) at 37 °C for 2 h. Stained cells were examined under a confocal microscope (FV10i, Olympus, Japan) for subcellular location of HERG protein.

2.5. Co-immunoprecipitation

HEK 293 cells were harvested 48 h post transfection in 1 ml ice-cold PBS, pelleted, and lysed in lysing buffer (0.5% NP-40, 50 mM Tris–HCl, 150 mM NaCl, pH 7.5) containing complete EDTA-free protease inhibitor cocktail tablets (Roche). The supernatant was collected and assayed for protein concentration using a NanoDrop Spectrophotometer (NanoDrop Technologies, DE, USA). Immunoprecipitation reactions containing 300–375 μg of total lysate protein were performed in a final volume of 300–350 μl. Reactions were incubated for overnight at 4 °C. Immunocomplexes were collected with Protein G-Agarose (Roche) for 2 h at 4 °C. Collected samples were washed three times with 800 μl lysing buffer, resuspended in 30 μl 5% β-mercaptoethanol/SDS buffer, and boiled 10 min to release the immunoprecipitated protein from the agarose beads. Eluted samples were analyzed by western blot assay.

2.6. Statistical analysis

Pooled data are presented as mean ± S.E.M. The statistical differences of paired or unpaired data were evaluated by Student's paired *t*-test or one-way repeated measures ANOVA followed by *q* test for mean value comparison when appropriate. A *P* value of <0.05 was considered significant.

3. Results

3.1. Electrophysiologic characteristics of A422T channel

First of all, whole-cell currents were recorded from HEK 293 cells transiently expressing wild-type (WT) or A422T mutant (A422T) channels alone without hMiRP1 to define the functional changes of the missense mutation A422T. The cells were depolarized to test voltages from −70 to +60 mV in 10 mV increments for 2 s from holding potential of −80 mV, followed by a voltage to −40 mV for 2 s to elicit step and tail currents (Fig. 1A, inset). Current recorded from WT channel showed relatively slow activation and deactivation with an inwardly rectifying profile, the typical HERG current traces (Fig. 1A, left panel). For A422T channels, however, no functional current was recorded (Fig. 1A, right panel).

To mimic the heterozygous status occurred in the patient and investigate whether A422T mutation exerts dominant-negative suppression on WT, HEK 293 cells were transiently transfected with 0.5 μg of WT together with varying amount of A422T (1, 4, 10 μg respectively). As shown in Fig. 1B, the currents from the cells co-expressing WT plus A422T decreased gradually with increasing amount of A422T cDNA, indicating a concentration-dependent dominant-negative effect. For the steady-state activation process, the peak current was generally obtained at a depolarizing step to +20 mV. As shown in Fig. 1B, the step current for A422T/WT (at a ratio of 1:1) at depolarization to +20 mV was 43.6 ± 0.9 pA/pF, and the tail current for A422T/WT measured at −40 mV after a depolarizing test pulse to +20 mV was 18.5 ± 5.5 pA/pF, indicating an obvious reduction in their amplitudes compared to WT alone ($P < 0.01$; Fig. 1C). Normalized amplitudes of tail current were plotted as a functional test potential and fitted with Boltzmann equation to generate activation curve (Fig. 1D). The $V_{1/2}$ for WT alone was −11.7 ± 2.1 mV with a slop factor of 8.6 ± 0.9, whereas that for A422T/WT was −26.3 ± 2.0 mV ($n = 9$) with a slope factor of 14.8 ± 1.5, respectively, indicating that the threshold voltage for A422T/WT to elicit current was significantly shifted to more negative potential ($P < 0.05$). In terms of inactive kinetics (Fig. 1E), the $V_{1/2}$ for WT was −49.2 ± 1.3 mV with a slope factor of 15.5 ± 0.3 and that for A422T/WT was −51.8 ± 1.9 mV with a slope factor of 20.8 ± 2.7 ($n = 8$); whereas the differences were not statistically significant ($P > 0.05$). Recovery from inactivation of HERG channel was also analyzed with a single exponential fitting to the initial phases of the recovery currents, yielding the time constants of recovery from inactivation. As illustrated in Fig. 1F, the τ values for time constant driven from A422T/WT channels were slightly increased at the voltage ranging from −70 mV to −50 mV compared to that obtained from WT channels. Although a trend in a slowdown of recovery from inactivation was observed in A422T/WT channels, it was not significantly different from WT.

3.2. Retention of missense mutation A422T proteins in ER

To examine the molecular mechanisms responsible for the mutant channel, expression of HERG proteins were analyzed by western blotting. WT channel protein on western blot was present in both immature core-glycosylated form of 135 kDa that is localized to the ER and mature complexly glycosylated form of 155 kDa

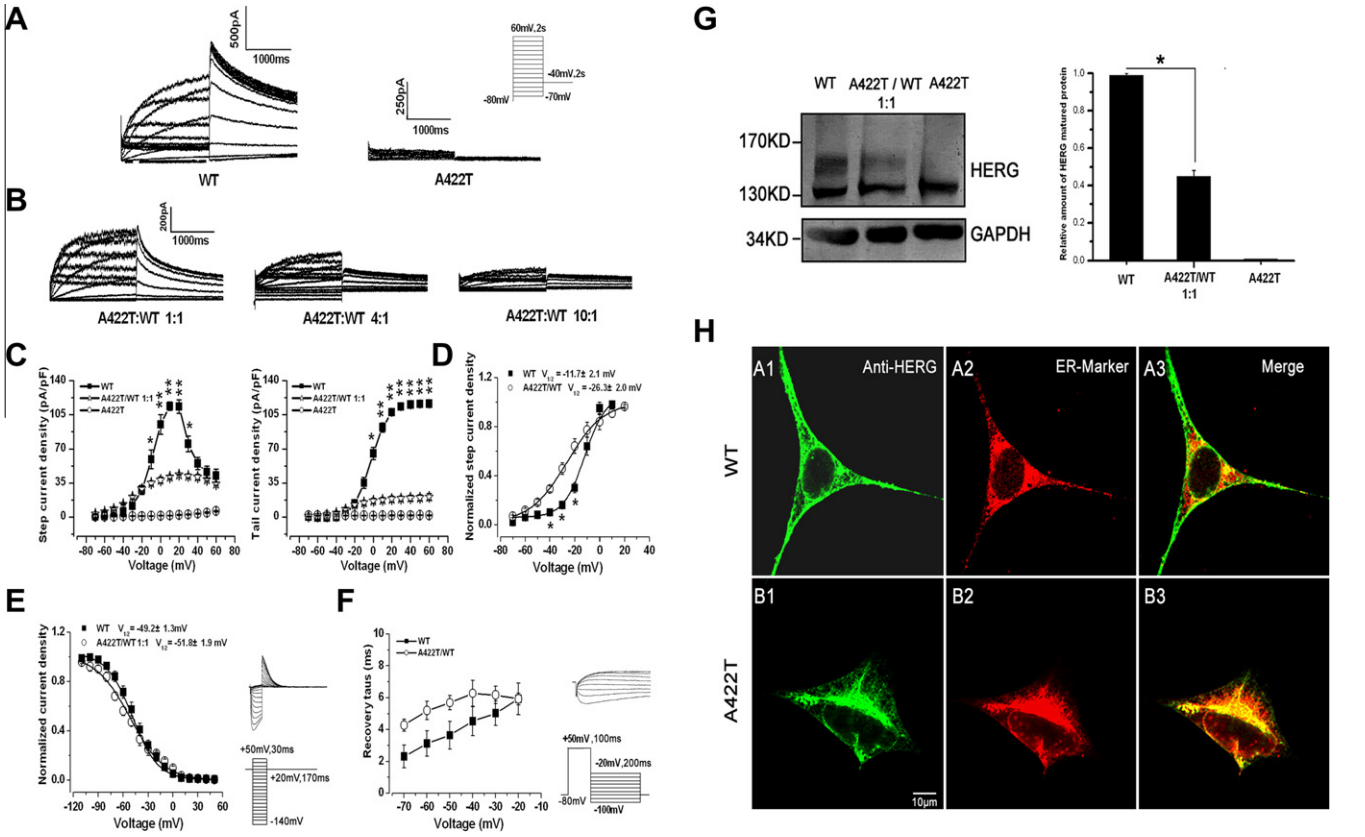

Fig. 1. The influence of A422T mutant on WT currents and expression. (A) Representative current traces recorded from HEK 293 cells expressed WT (left) or A422T (right) with the pulse protocol shown in the inset for assessing voltage-dependence of channel activation. (B) Example of recording traces from HEK 293 cells transfected with plasmids of A422T and WT at different ratios (1:1, 4:1, 10:1), illustrating that with the increase in amount of A422T, the current significantly decreased. (C) Current–voltage relationship for step (left) and tail (right) current densities in comparison among WT, A422T/WT (1:1) and A422T (*$P < 0.05$; **$P < 0.01$ WT vs. A422T/WT, $n = 9$). (D) Steady-state activation curve generated by plotting normalized tail currents as a function of test potentials with the fits to Boltzmann function for WT (filled square, $n = 9$) and A422T/WT channel (open circle, $n = 9$). A significant leftward shift of activation process was documented for A422T/WT as compared to WT alone (*$P < 0.05$). (E) The steady-state inactivation curves measured with a two-pulse protocol (see inset) were illustrated for WT (filled square, $n = 12$) and A422T (open circle, $n = 10$). Outward current amplitudes induced by second step to +20 mV were measured, and normalized values were plotted as a function of the preceding test potentials with the fits to Boltzmann equation. No significant difference was observed between WT and A422T/WT ($P > 0.05$). Half-maximal voltage values ($V_{1/2}$) for I_{HERG} steady activation or inactivation were obtained by fitting normalized appropriate currents with a Boltzmann distribution equation, $I/I_{max} = 1/\{1/exp[(V_{1/2} - Vm)/k$ using software Origin 6.0 for Windows as previously described. (F) Recovery from inactivation was assessed by a pulse protocol shown in the inset. Time courses of recovery from inactivation at the voltage arrange from −70 to −20 mV were slightly slower in A422T/WT channels than that in WT alone and the differences between them, however, were not statistically significant ($P > 0.05$, $n = 6$). These mean A422T mutant exerted a dominant negative suppression on WT currents in a concentration-dependent manner. (G) Representative western blot analysis of WT, A422T, and A422T/WT (1:1) protein (left) followed by quantification from 3 separate experiments. Data were presented as matured proteins of A422T/WT or A422T alone relative to that of WT. The difference between A422T/WT and WT was significant. *$P < 0.05$. H, immunofluorescent staining for HEK 293 cells expressing WT or A422T. Confocal imagines were taken from the cells expressing WT and A422T, respectively. The left column (A1 vs. B1) indicates the channel protein labeled with rabbit polyclonal anti-HERG (1:50 dilution, Alomone) as primary antibody, and Alexa Flour 488 (in green) goat anti-rabbit IgG (H + L) as the second antibody. The middle column (A2 vs. B2) illustrates the ER by labeling with mouse monoclonal anti-calnexin (1:100 dilution, Abcam), followed by incubation with Alexa Flour 555 (in red) goat anti-mouse IgG (H + L). Right column (A3 vs. B3) displays the superimposed two color imagines. Calibration bar shown in B1 = 10 μm. Expression and subcellular localization of WT channel protein was changed. (For interpretation of the references to colour in this figure legend, the reader is referred to the web version of this article.)

which would be inserted into the cell membrane [7,10]. In contrast to WT, only the band at 135 kDa was seen for the A422T alone. In the case of A422T/WT, two protein bands appeared, but the mature form of A422T/WT expressed less well than WT alone and more than A422T alone, confirming a dominant-negative effect resulted from trafficking defects in A422T protein (Fig. 1G).

To further investigate the consequence of A422T mutation, subcellular localization of mutant proteins in the cell surface and cytoplasm was examined. The HEK293 cells expressing WT or A422T were double stained with anti-HERG antibodies that recognized the S1–S2 external linker region of the HERG channel (Alomone) and anti-calnexin (the ER marker protein calnexin) antibodies (Abcam). The localization of labeled HERG proteins or labeled calnexin was visualized by incubating the permeabilized cells with Alexa Fluor 488-conjugated or Alexa Fluor 555-conjugated secondary antibody, respectively. The cells expressing WT showed marked surface membrane localization of HERG; whereas the cells expressing A422T apparently had an abnormal intracellular granular pattern with reduced fluorescent intensity on membrane surface (Fig. 1H, A1 vs. B1). Notably, the intense cytoplasmic staining of HERG in cells expressing A422T was well overlapped with calnexin (Fig. 1H, A2 vs. B2), suggesting a co-localization between A422T and ER resident transmembrane protein calnexin (Fig. 1H, B3). These results documented that the maturation defect in A422T protein led to its ER retention.

3.3. Rescuing effects of chemical chaperon and low temperature on the trafficking of A422T

It has been reported that several trafficking-deficient mutations residing in different regions of the HERG protein, such as G601S, N470D, and R752W, seem to be the key components in determining temperature-dependent or chemical chaperone-dependent rescuing effects. To examine whether that is the case for A422T

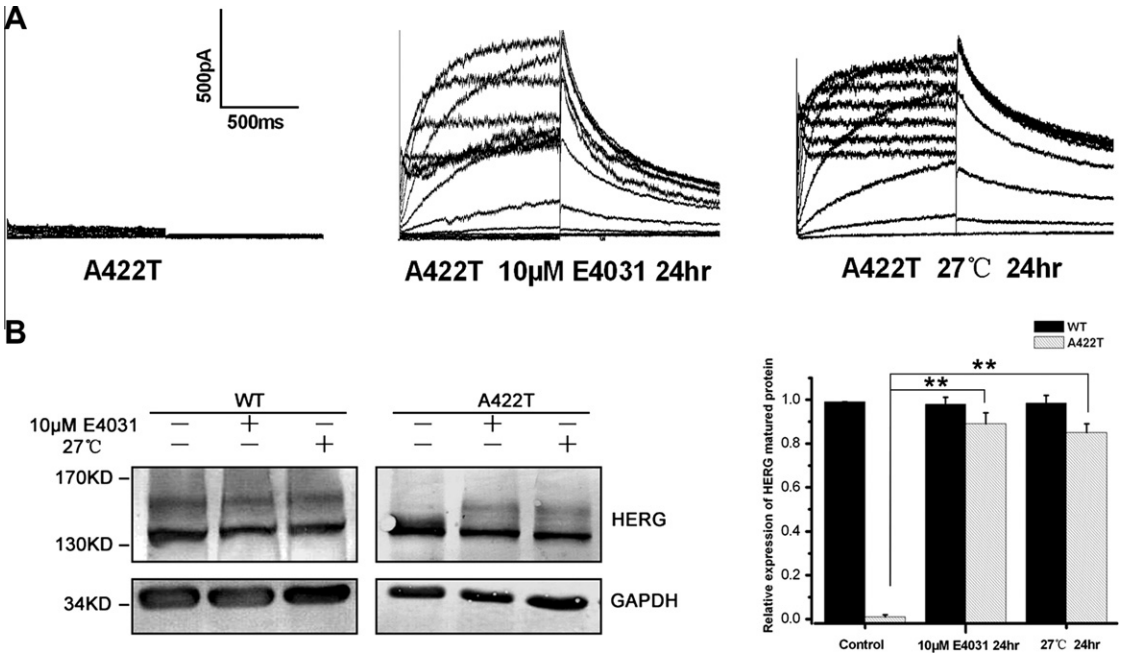

Fig. 2. The rescue effects of E4031 or lower incubation temperature on A422T mutation. (A) No current was produced from A422T channel (left) but functional currents were elicited after administration of E4031 (middle) for 24 h or incubation at 27 °C (right). (B) Representative western blot analysis of the protein expression under the different conditions (as labeled at the bottom) followed by quantitation from 3 independent experiments. The data were presented as relative matured protein of A422T to WT. Data were presented as matured proteins of A422T under different conditions relative to that of A422T. The difference between them was significant. $^{**}P < 0.01$.

mutant, the protein expression and functional assays were performed. The results showed that currents recorded from the cells expressing A422T were partially rescued upon treatment with E4031 (10 μM) or lowering temperature to 27 °C for 24 h (Fig. 2A). Correspondingly, the matured protein of A422T was increased, inferred by the appearance of the 155-kDa protein in western blot analysis (Fig. 2B). These results demonstrated that E4031 or lower incubation temperature could restore both A422T channel function and protein expression.

3.4. The role of chaperon protein Hsp70 or Hsp90 in A422T trafficking

In mammalian cells, the Hsp70/Hsp90 network is known to be important for polypeptide folding, sorting, transport and degradation [4,11]. The recovery of channel trafficking and function by temperature reduction or pharmacological stabilization was tightly coupled to the formation of channel-chaperone complexes. Hence, the concrete effects of Hsp70 or Hsp90 on the HERG protein trafficking and functional currents were then examined. First,

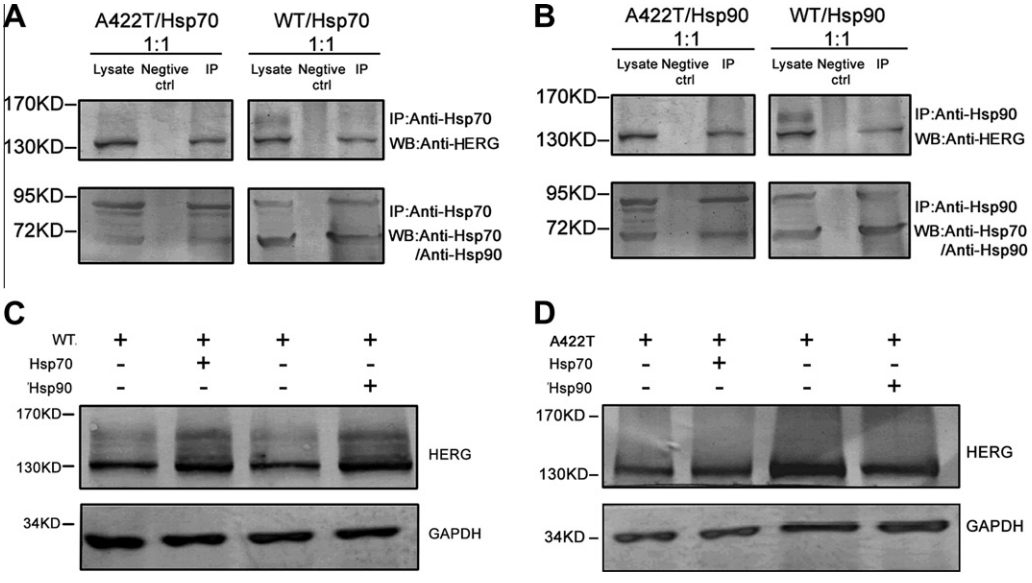

Fig. 3. The effects of Hsp70 or Hsp90 overexpression on HERG channel protein. (A)Lysates of HEK 293 cells transiently transfected with A422T (left) and WT (right) were immunoprecipitated with anti-Hsp70 antibody. Membranes were blotted with anti-HERG (top), anti-Hsp70 or anti-Hsp90 (bottom) visualizations, respectively. (B) HEK 293 cells were transiently transfected with either A422T or WT, lysed, and immunoprecipitated with anti-Hsp90 antibody as indicated. Membranes were blotted with anti-HERG, anti-Hsp70 or anti-Hsp90 antibody for visualization. Normal mouse IgG (Santa Cruz) was used as a negative control instead of antibodies for immunoprecipitation. (C) and (D) illustrate representative Western blot analysis of the protein expression in cells co-expressing WT and Hsp70 or Hsp90 (left) and in cells co-expressing A422T and Hsp70 or Hsp90 (right).

co-immunoprecipitation experiments were conducted to determine the association of HERG protein with Hsp70 or Hsp90. The cells transfected with WT/Hsp70, WT/Hsp90, A422T/Hsp70 or A422T/Hsp90 plasmids were lysed, and immunoprecipitated with the antibody against Hsp70 or Hsp90, respectively. As shown in Fig. 3A and B, the formation of WT-Hsp70/Hsp90 or A422T-Hsp70/Hsp90 complexes were detectable by co-immunoprecipitation with Hsp70 or Hsp90 antibodies. Interestingly, two chaperon proteins, both Hsp70 and Hsp90, apparently interacted exclusively with core-glycosylated immature HERG protein, but not with the full-glycosylated mature one. For the WT, the levels of both mature and immature forms of protein were increased under the condition of either co-expression with Hsp70 or Hsp90 (Fig. 3C). In contrast, an immature band at 135 kDa only was found from A422T mutant (Fig. 3D).

Next, the currents were recorded from the cells which co-expressed molecular chaperones with WT or A422T. Fig. 4 was a representative set of current recording data under different conditions. As shown in Fig. 4A and B, the amplitudes of currents recorded from WT were enhanced in response to either co-expression of Hsp70 or Hsp90; whereas no proper currents were generated from A422T mutant (Fig. 4C) upon co-expression of Hsp70, even though the ratio of Hsp70 was increased (Fig. 4D). Surprisingly, small amplitude currents but with a gating behavior similar to the WT were obtained from the cells co-expressing A422T and Hsp90 (Fig. 4E left). To verify the role of Hsp90 in current generation, cells co-expressed A422T and Hsp90 were cultured for 24 h in DMEM containing 2 μM celastrol, an inhibitor of Hsp90. As expected, Hsp90-related current restoration was abolished in the presence of celastrol (Fig. 4E right panel). Moreover, it was observed that current amplitudes from the cells co-expressing A422T/ Hsp90 were not further increased by the addition of Hsp70 expression (Fig. 4F), suggesting the crucial role of Hsp90 in restoration of A422T currents although both Hsp70 and Hsp90 might have participated in the process of HERG trafficking.

4. Discussion

Abnormal trafficking of the mutant protein is thought to be involved in its mis-folding or improper assembly, leading to the retention in the ER by the "quality control" system [11,12]. The results of the present study indicated that A422T mutation produced an immature form of the protein and A422T mutant affected the expression of mature WT channel proteins and gating behavior. A422T mutation was in the S1 segment of HERG channel and it is just next to another LQT2 mutation, T421M, which affects gating but does not cause trafficking defect [13]. Our results also suggest that the A422 may be involved in stabilizing open gating states.

Similar to other LQT2 causing mutations with trafficking defect, such as G601S, K28E, and N407D, A422T mutation was partially restored by treatment with E4031 or incubation at 27 °C. In respect of tail currents, A422T mutant in the presence of E4031 produced functional currents, which increased more than 16.5-fold in the current density. It has been reported that pharmacologic rescue of some HERG channel blockers requires binding of these blockers to the inner vestibule of the assembled tetrameric HERG channel, implying that only the proteins that are able to assemble into tetramers are possibly stabilized by the blockers [14]. Based on those, we considered A422T as a mild mis-folded protein which is able to be assembled into tetramers, but needs to be stabilized by E4031 or other blockers.

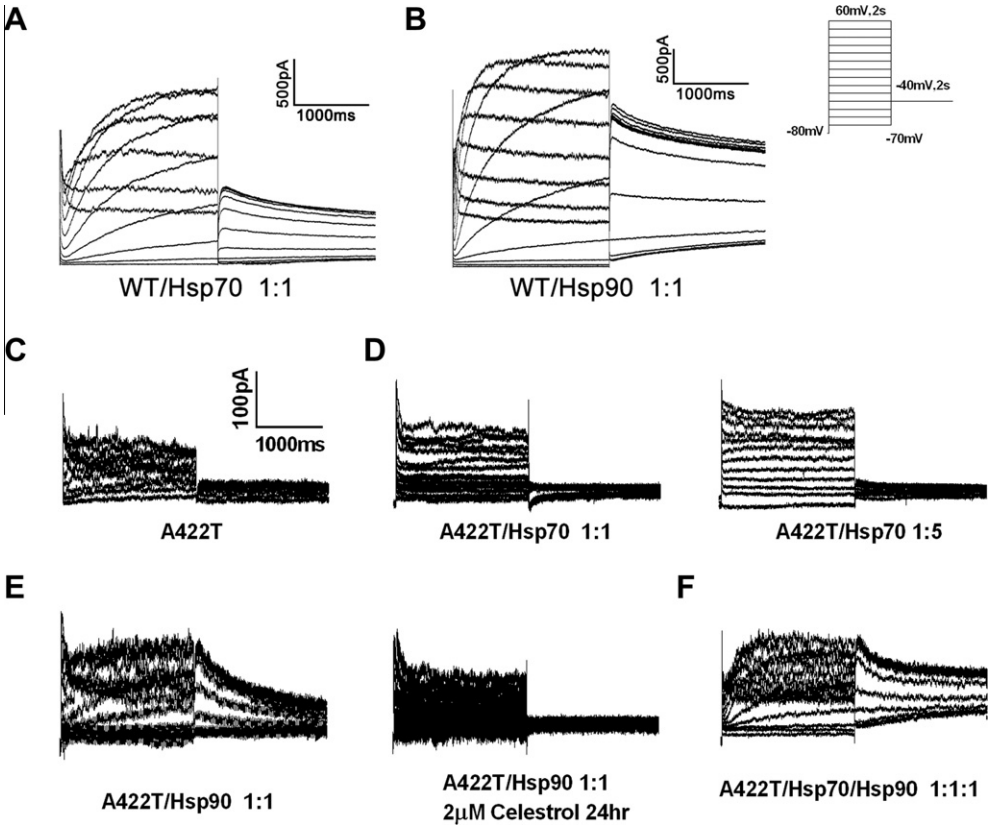

Fig. 4. The effects of Hsp70 or Hsp90 on the currents of HERG channel. Representative current traces recorded from the cells expressing WT plus Hsp70 (1:1; panel A) or Hsp90 (1:1; panel B), the cells expressing A422T plus Hsp70 with different ratios (1:1 or 1:5; panel C and D), cells expressing A422T plus Hsp90 at a ratio of 1:1 before (left) and after (right) addition of celastrol, an inhibitor of Hsp90 (panel E) and the cells co-expressing A422T plus Hsp70 and Hsp90 (F). The traces in C–F exhibited in the same scale bar as indicated in panel C.

Many chaperone molecules, such as Hsp70/Hsc70, Hsp90 or FK506-binding protein (FKBP38), interact with HERG to facilitate its proper folding [10]. More recently, the observation of reciprocal control of HERG stability by Hsp70 and Hsc70 reported by Li et al. [15] clarified further crucial role of molecular chaperons for the maturation of WT as well as the retention of trafficking-deficient LQT2 mutants. In accordance with these studies, we showed that expression in both mature and immature proteins as well as current densities for WT were increased along with overexpression of Hsp70 and Hsp90, in spite of the interaction of Hsp70 or Hsp90 with immature HERG protein. However, Hsp70 and Hsp90 may have different effects on A422T current restoration. The cells co-expressing of Hsp90 with A422T mutant are capable of generating currents, which coexisted with a similar kinetic property as that of WT although its amplitude is small. Interestingly, negative shift in an activation process is corrected by Hsp90. In contrast, such an effect was not observed in the cells co-expressing Hsp70 with A422T mutant. The difference in functional correction might be explained by a proposed sequential chaperone pathway for the folding of HERG, in which Hsp70 acts at an early stage as forming complexes with HERG folding intermediates when either folding or degradation is a possible outcome [16]. Given the fact that the interactions of A422T with Hsp70 or Hsp90 occur together but the improvement of trafficking happen only with Hsp90, it is likely that mild mis-folding A422T is somehow capable of bypassing earlier stages of the chaperon pathway and then transferring themselves onto Hsp90 via other chaperons. The condition of over-expressing Hsp90 may favor the chaperon balance towards HERG folding, with a result that A422T exits from ER. Although our results showed no notable mature protein band paralleled to the restored current, it is possible that our detecting system is not sensitive enough to recognize the tiny changes of protein expression in cells overexpressing Hsp90. Nevertheless, it is no doubt that Hsp90 plays a prominent role in A422T trafficking. Further studies are needed to investigate the dynamic interaction of the mutant protein with Hsp90, the role of other components involved in chaperon pathways for A422T trafficking, and the fate of A422T that was remained in ER under the condition of over-expressing or knockdown of Hsp70 or Hsp90.

In summary, the findings in this study show that the functional loss caused by A422T mutation in HERG K^+ channel is attributed to protein trafficking defect with ER retention. And chemical or pharmacologic agents could partly rescue functional loss of A422T mutant channel. Our findings indicate that small molecule approaches would to be used as arrhythmia treatment to correct trafficking defects.

Conflict of interest

Authors state no conflicts of interest.

Acknowledgments

We thank Dr. Nipavan Chiamvimonvat and Dr. Gail A. Robertson for providing us the plasmids of HERG and Dr. Zhimin Yin for providing us the plasmids of pCDNA3-Hsp70 and pCDNA3-Hsp90. This work was supported by the National Natural Science Foundation (No. 30570662, No.30871228 to Dr. Zhao Zhang), by Outstanding Doctoral Students Fund from Nanjing Normal University, Graduate Research Innovation Fund from Jiangsu Province (No.1243211601159, No.181200000658, to Jia Guo) and by the Priority Academic Program Development of Jiangsu Higher Education Institutions (No.164320H106). In addition, it was partially supported by the National Key Basic Research Program (2006CB943503 to Dr. Zhao Zhang) from Ministry of Science and Technology of P. R. China.

References

[1] M.C. Sanguinetti, M. Tristani-Firouzi, HERG potassium channels and cardiac arrhythmia, Nature 440 (2006) 463–469.
[2] M.C. Sanguinetti, C. Jiang, M.E. Curran, M.T. Keating, A mechanistic link between an inherited and an acquired cardiac arrhythmia: HERG encodes the IKr potassium channel, Cell 81 (1995) 299–307.
[3] M.J. Perrin, R.N. Subbiah, J.I. Vandenberg, A.P. Hill, Human ether-a-go-go related gene (hERG) K+ channels: function and dysfunction, Prog. Biophys. Mol. Biol. 98 (2008) 137–148.
[4] G.N. Tseng, I(Kr): the hERG channel, J. Mol. Cell. Cardiol. 33 (2001) 835–849.
[5] D. Sharma, K.A. Glatter, V. Timofeyev, D. Tuteja, Z. Zhang, J. Rodriguez, et al., Characterization of a KCNQ1/KVLQT1 polymorphism in Asian families with LQT2: implications for genetic testing, J. Mol. Cell. Cardiol. 37 (2004) 79–89.
[6] G.W. Abbott, F. Sesti, I. Splawski, M.E. Buck, M.H. Lehmann, K.W. Timothy, et al., MiRP1 forms IKr potassium channels with HERG and is associated with cardiac arrhythmia, Cell 97 (1999) 175–187.
[7] Z. Zhou, Q. Gong, B. Ye, Z. Fan, J.C. Makielski, G.A. Robertson, et al., Properties of HERG channels stably expressed in HEK 293 cells studied at physiological temperature, Biophys. J. 74 (1998) 230–241.
[8] J. Guo, S.N. Han, J.X. Liu, X.M. Zhang, Z.S. Hu, J. Shi, et al., The action of a novel fluoroquinolone antibiotic agent antofloxacin hydrochloride on human-ether-a-go-go-related gene potassium channel, Basic Clin. Pharmacol. Toxicol. 107 (2010) 643–649.
[9] Y.V. Liu, J.H. Baek, H. Zhang, R. Diez, R.N. Cole, G.L. Semenza, RACK1 competes with HSP90 for binding to HIF-1alpha and is required for O(2)-independent and HSP90 inhibitor-induced degradation of HIF-1alpha, Mol. Cell 25 (2007) 207–217.
[10] E. Ficker, A.T. Dennis, L. Wang, A.M. Brown, Role of the cytosolic chaperones Hsp70 and Hsp90 in maturation of the cardiac potassium channel HERG, Circ. Res. 92 (2003) e87–100.
[11] D. Thomas, J. Kiehn, H.A. Katus, C.A. Karle, Defective protein trafficking in hERG-associated hereditary long QT syndrome (LQT2): molecular mechanisms and restoration of intracellular protein processing, Cardiovasc. Res. 60 (2003) 235–241.
[12] S.Y. Balijepalli, C.L. Anderson, E.C. Lin, C.T. January, Rescue of mutated cardiac ion channels in inherited arrhythmia syndromes, J. Cardiovasc. Pharmacol. 56 (2010) 113–122.
[13] D.J. Tester, M.L. Will, C.M. Haglund, M.J. Ackerman, Compendium of cardiac channel mutations in 541 consecutive unrelated patients referred for long QT syndrome genetic testing, Heart Rhythm 2 (2005) 507–517.
[14] E. Ficker, C.A. Obejero-Paz, S. Zhao, A.M. Brown, The binding site for channel blockers that rescue misprocessed human long QT syndrome type 2 ether-a-gogo-related gene (HERG) mutations, J. Biol. Chem. 277 (2002) 4989–4998.
[15] P. Li, H. Ninomiya, Y. Kurata, M. Kato, J. Miake, Y. Yamamoto, et al., Reciprocal control of hERG stability by Hsp70 and Hsc70 with implication for restoration of LQT2 mutant stability, Circ. Res. 108 (2011) 458–468.
[16] V.E. Walker, M.J. Wong, R. Atanasiu, C. Hantouche, J.C. Young, A. Shrier, Hsp40 chaperones promote degradation of the HERG potassium channel, J. Biol. Chem. 285 (2010) 3319–3329.